




Isotope effects on cubic boron nitride investigated by x-ray scattering

Hiroshi Fukui (福井宏之) ^{1,2,*}, Daisuke Ishikawa (石川大介),^{1,2} Taishun Manjo (萬條太駿) ^{1,2},
Nozomu Hiraoka (平岡望),³ Takashi Taniguchi (谷口尚),⁴ and Alfred Q. R. Baron ^{1,2}

¹Materials Dynamics Laboratory, RIKEN SPring-8 Center, Kouto 1-1-1, Sayo, Hyogo 679-5148, Japan

²Precision Spectroscopy Division, Japan Synchrotron Radiation Research Institute, Kouto 1-1-1, Sayo, Hyogo 679-5198, Japan

³National Synchrotron Radiation Research Center, Hsinchu 30076, Taiwan

⁴National Institute for Materials Science, Namiki 1-1, Tsukuba, Ibaraki 305-0044, Japan



(Received 25 August 2023; revised 27 September 2023; accepted 12 October 2023; published 31 October 2023)

We have investigated effects of boron isotope enrichment of cubic boron nitride (cBN). X-ray Raman scattering spectra of ^{10}B and ^{11}B enriched samples did not show any chemical shift. meV-resolved inelastic x-ray scattering was used to measure the phonon dispersion. The shift of phonon frequencies between a sample with the natural abundance of B (20% ^{10}B) and a sample nearly 100% enriched in ^{10}B was reasonably explained by treating the mass difference with the same force constants—i.e., purely an isotope effect. The observed shifts were also consistent with first-order perturbation theory which gives the frequency shift, $\Delta\omega_j$, as $\frac{\Delta\omega_j}{\omega_j} = -\frac{1}{2} \frac{\Delta M_d}{M_d} \mathbf{e}_{jd}^* \cdot \mathbf{e}_{jd}$, where M_d , ΔM_d , \mathbf{e}_{jd} , and ω_j are the atomic mass, change in mass, the eigenvector, and the phonon angular frequency for atom d and phonon mode j , respectively.

DOI: [10.1103/PhysRevB.108.134311](https://doi.org/10.1103/PhysRevB.108.134311)

I. INTRODUCTION

Insulators with ultrahigh thermal conductivity attract the interest of researchers in fundamental and applied physics. It was demonstrated that thermal conductivity of ^{10}B or ^{11}B isotope-enriched cubic boron nitride (cBN) was $\sim 1600 \text{ W m}^{-1} \text{ K}^{-1}$, almost two times larger than that of cBN with the natural isotope abundances ($\sim 850 \text{ W m}^{-1} \text{ K}^{-1}$) [1]. The effect of nitrogen isotope enrichment was not evaluated since the natural abundances of nitrogen are 99.6% of ^{14}N and 0.4% of ^{15}N , whereas those of boron are 19.9% of ^{10}B and 80.1% of ^{11}B . Based on calculations, Chen *et al.* suggested that the enhancement of the thermal conductivity by isotope enrichment in cBN was the result of large phonon-isotope scattering in cBN with natural isotope abundances [1]. Phonon properties for cBN have not been experimentally determined to our best knowledge except for the Raman spectra. It is important to confirm phonon-dispersion relations experimentally. Though inelastic neutron scattering (INS) is often used to measure them, it is almost impossible to grow good-quality single crystals of cBN into a size large enough for INS measurements.

We have performed inelastic x-ray scattering measurements on cBN single-crystal samples. Samples were evaluated using x-ray Raman scattering (XRS) and x-ray diffraction. Phonon properties are measured using millielectronvolt-resolved inelastic x-ray scattering (meV-IXS) [5]. Based on phonon spectra, we discuss the effect of isotope enrichment on the thermal conductivity of cBN.

II. METHODS

Samples were cubic boron nitride crystals combining natural abundant nitrogen with different boron isotope compositions. The samples with natural isotope abundances were synthesized by a temperature-gradient method using a solvent under high pressure, and the crystals were of high quality [2,3]. The isotope-enriched samples were obtained directly from a metathesis reaction (Taniguchi (unpublished); some information will be found in Ref. [1]). The isotope compositions considered were $>99\%$, $\sim 19.9\%$, and $<1\%$ of ^{10}B for $c^{10}\text{BN}$, $c^{\text{nat}}\text{BN}$, and $c^{11}\text{BN}$, respectively. Colorless and transparent grains having smooth surfaces were selected for x-ray measurements. The samples were planar and the sizes were $100 \sim 300 \mu\text{m}$ for two sides and $50 \sim 100 \mu\text{m}$ for another.

We evaluated the electronic structures of $c^{10}\text{BN}$ and $c^{11}\text{BN}$ by XRS, which was performed at BL12XU of SPring-8 [4]. If isotope enrichment affected the electronic structure, the difference should appear between ^{10}B and ^{11}B . The incident x-ray energy was tuned to 9886 eV. The energy resolution was 1.4 eV full width at half maximum (FWHM). The scattering angle was 30° .

meV-IXS measurements were carried out at BL43LXU of SPring-8 [5,6]. The samples were $c^{10}\text{BN}$ and $c^{\text{nat}}\text{BN}$. The reason we measured not $c^{11}\text{BN}$ but $c^{10}\text{BN}$ is that a higher contrast with $c^{\text{nat}}\text{BN}$ was expected. The spectrometer was operated at 17.747 keV with the focusing beam ($5 \times 4 \mu\text{m}^2$ for horizontal \times vertical FWHM) [7]. The energy resolution was 2.8-meV FWHM and the momentum resolution was set to $\sim 1.0 \text{ nm}^{-1}$ with the slit system in the front of the analyzer crystals. Obtained spectra were analyzed using smoothly approximated resolution functions [8].

We also performed first-principles calculations with plane-wave basis to evaluate phonon polarizations as well as phonon frequencies for cBN. They were performed using

*fukuhi@spring8.or.jp

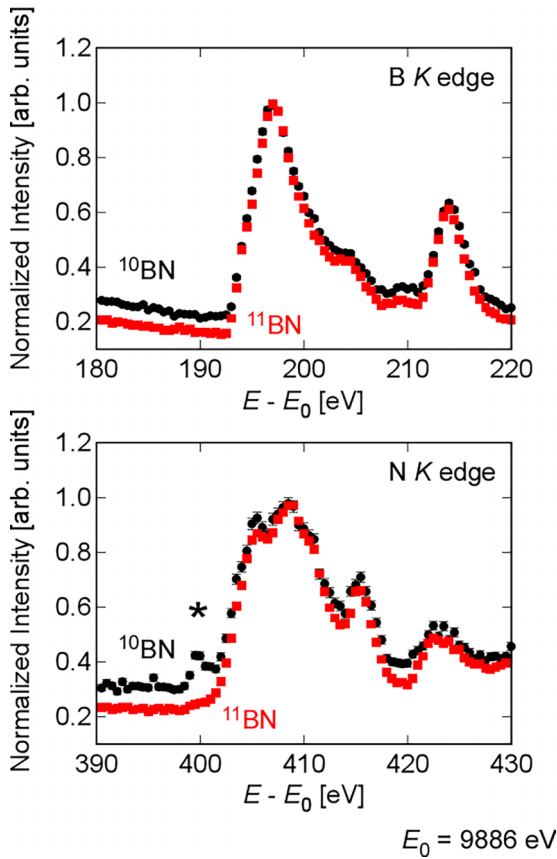


FIG. 1. B K - (top) and N K - (bottom) edge XRS spectra for cBN crystals. Black and red symbols indicate data points for $c^{10}\text{BN}$ and $c^{11}\text{BN}$ samples, respectively. Peak with asterisk in N K -edge spectrum for $c^{10}\text{BN}$ can be considered as π^* level of hBN.

QUANTUM ESPRESSO package [9]. The pseudopotentials were constructed with the ultrasoft-pseudizing method [10] in the local-density approximation [11]. Nonlinear core correction and scalar relativistic effects were taken into account. The energy cutoff and convergence threshold were 140 and 10 Ry, respectively. K mesh for the electronic energy sampling was $12 \times 12 \times 12$ with shift. Phonon energy calculation based on density-functional perturbation theory (DFPT) was performed at $4 \times 4 \times 4$ mesh of q points. The mass for B was 10.00 or 10.81 and that for N was 14.007. Using interatomic force constant matrices based on the DFPT calculations, IXS spectra were also simulated. The detail of the simulation is given elsewhere [12].

III. RESULTS AND DISCUSSION

XRS spectra of the samples are shown in Fig. 1. Comparing with x-ray absorption near-edge structure/electron-energy-loss spectroscopy spectra in previous studies [13,14], these spectra indicate that the samples mainly consisted of the cubic phase. Note that the N K -edge spectrum of $c^{10}\text{B}$ showed a small peak at 400 eV (indicated with an asterisk in Fig. 1). This is consistent with the π^* peak of the hexagonal phase [13], indicating a small amount of hBN was present. The slightly higher background for the $c^{10}\text{BN}$ sample is probably due to impurities. In conclusion, there is no significant

difference in the B K -edge spectra as well as the N K -edge ones between the $c^{10}\text{BN}$ and $c^{11}\text{BN}$ samples with respect to the peak energies and intensity ratios: both $c^{10}\text{BN}$ and $c^{11}\text{BN}$ have the identical electronic structure with respect to the XRS spectra.

X-ray oscillation photographs of the samples were made before the IXS measurements. The photos for $c^{10}\text{BN}$ samples showed several diffraction spots, all of which could not be indexed using a single UB matrix, suggesting multiple grains were present. In contrast, the $c^{\text{nat}}\text{BN}$ sample was a single domain. The results of XRS and the oscillation photography are consistent with the fact that the single-crystal syntheses of isotope-enriched cBN through a metathesis reaction is essentially difficult to get a single-crystal due to the mixture of spontaneous nucleation and growth. Single crystals should be obtained by shaping by precision polishing, etc., but this is difficult with cBN, which is a very hard material and the crystals in this study are small. In order to obtain a large-isotope pure cBN crystals, we need to use Ba-BN base solvent for a crystal growth. In this case, natural isotope boron will be contaminated into the grown cBN crystal with isotopically pure BN source as a starting material. Note that the multiple grains as well as a minor phase of hBN did not impact the interpretation of phonon signals of cBN.

Figure 2 shows comparison of IXS spectra with the $c^{\text{nat}}\text{BN}$ and $c^{10}\text{BN}$ samples which were measured at the same q points. Calculated IXS spectra are also shown for comparison. Most of all excitations can be interpreted based on the orientation matrix for the main grain. The intensity difference may be due to the low statistics of the experimental spectra. The spectra of the $c^{10}\text{BN}$ sample show (quasi-)elastic intensity and small inelastic peaks which cannot be explained with a single domain. These indicate the relatively poor crystal quality of the $c^{10}\text{BN}$ sample and are consistent with other results.

The phonon energies at phonon momenta for the $c^{\text{nat}}\text{BN}$ and $c^{10}\text{BN}$ samples are shown in Fig. 3 together with calculated phonon-dispersion relations. The calculation curves reasonably reproduced the experimental data though the frequencies for transverse optical modes were slightly underestimated in the calculations. Tables I and II show the phonon energies and linewidths from the fitting together with phonon momenta, respectively. For pairs of phonon modes with the same irreducible expression and momentum, calculated energy ratios are also given in Table I as well as those from the DFPT calculations.

In the case that one atom in a primitive cell is replaced by another atom with a different mass, the application of first-order perturbation theory to the dynamical equation gives the isotope effect to the phonon frequencies as

$$\frac{\Delta\omega_j}{\omega_j} = -\frac{1}{2} \frac{\Delta M_d}{M_d} \mathbf{e}_{jd}^* \cdot \mathbf{e}_{jd}, \quad (1)$$

where M_d , ΔM_d , \mathbf{e}_{jd} , and ω_j are the atomic mass, change in mass, the eigenvector, and the phonon angular frequency for atom d and phonon mode j , respectively, and the eigenvectors are assumed to be normalized so that $\sum_d \mathbf{e}_{jd}^* \cdot \mathbf{e}_{jd} = 1$. Table I shows the energy ratio based on Eq. (1) using only the $c^{10,81}\text{BN}$ results from the DFPT calculations. The ratios from Eq. (1) show better agreement with the experimental results as well as those from two sets of the calculations with $^{10,81}\text{B}$

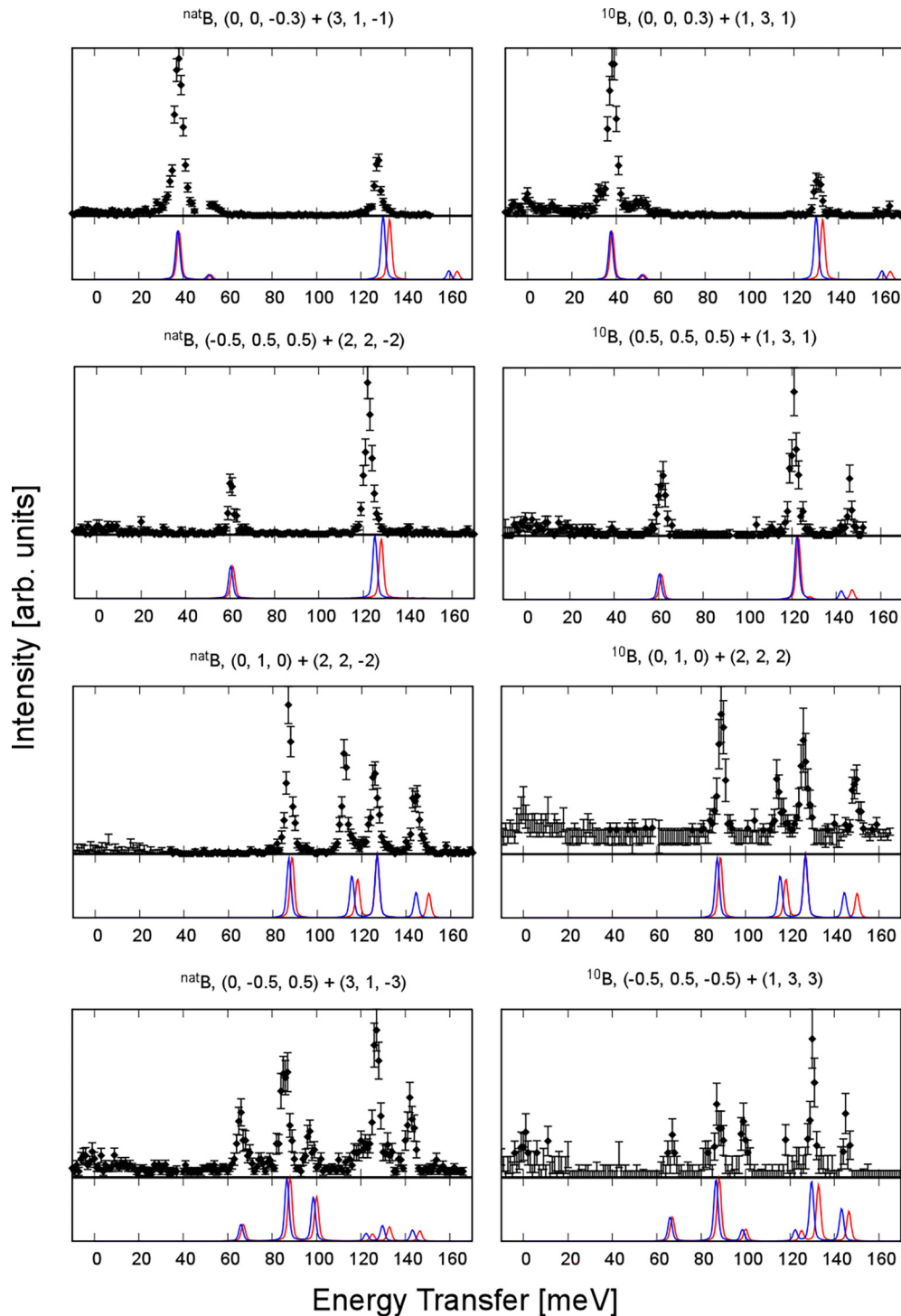


FIG. 2. IXS spectra (black circles) for $^{\text{nat}}\text{B}$ (left panels) and ^{10}B (right panels) samples. Blue and red lines are calculated IXS spectra for $^{10.81}\text{B} \ ^{14.007}\text{N}$ and $^{10}\text{B} \ ^{14.007}\text{N}$, respectively.

and ^{10}B than the simple correction in the arithmetic/harmonic mean masses does.

Isotope-enriched cBN samples reportedly showed very high thermal conductivity (Chen, 2020). The value for $c^{10}\text{BN}$ (as well as $c^{11}\text{BN}$) is about twice that for $c^{\text{nat}}\text{BN}$. The mode thermal conductivity is approximated as proportional to the product of the square of the phonon group velocity and the phonon lifetime based on the linearized phonon Boltzmann

transport equation (e.g., see Ref. [15]). As the ratio in phonon group velocities should be that of phonon energy, the number of $c^{10}\text{BN}$ to $c^{\text{nat}}\text{BN}$ is 1.04 at most as given in Table I. Therefore, the ratio of the phonon lifetime should be larger than 1.85.

We would like to consider whether the phonon lifetime in cBN may be determined using IXS. According to Chen *et al.* [1], the intrinsic 3-phonon scattering rate of acoustic

TABLE I. Experimentally determined phonon energies along high-symmetry lines. Phonons at the same q point are given close together (divided by thick lines). The values in bold are of acoustic modes.

H	K	L	h	k	l	E [meV]					sample	
2	2	-2	1	0	0	86.7 ± 0.1	112.1 ± 0.2	125.4 ± 0.2	143.7 ± 0.2	-	c ^{nat} BN	
3	1	1	1	0	0	89.2 ± 0.4	115.0 ± 0.6	126.3 ± 0.5	149.6 ± 0.4	-	c ¹⁰ BN	
			E_{10B}/E_{natB} (experiment)				1.028(6)	1.026(6)	1.007(5)	1.041(5)	-	
			E_{10B}/E_{natB} (DPFT)				1.022	1.022	1.000	1.040	-	
			E_{10B}/E_{natB} (Eq.)				1.021	1.021	1.000	1.041	-	
3	1	-1	0	0	-0.3	37.8 ± 0.1	53.7 ± 0.5	127.5 ± 0.1	-	-	c ^{nat} BN	
3	1	1	0	0	0.3	37.9 ± 0.1	50.8 ± 0.6	130.5 ± 0.2	162.0 ± 0.7	-	c ¹⁰ BN	
			E_{10B}/E_{natB} (experiment)				1.002(5)	0.946(20)	1.024(3)	-	-	
			E_{10B}/E_{natB} (DPFT)				1.017	1.016	1.022	-	-	
			E_{10B}/E_{natB} (Eq.)				1.021	1.020	1.025	-	-	
3	1	-1	-0.5	0.5	0.5	60.6 ± 0.6	122.3 ± 0.7	-	-	-	c ^{nat} BN	
4	0	0	-0.5	0.5	0.5	60.8 ± 0.1	120.7 ± 0.2	139.4 ± 1.2	-	-	c ^{nat} BN	
3	1	1	0.5	0.5	0.5	61.5 ± 0.5	121.1 ± 0.5	146.2 ± 0.5	-	-	c ¹⁰ BN	
			E_{10B}/E_{natB} (experiment)				1.014(14)	0.997(7)	1.048(13)	-	-	
			E_{10B}/E_{natB} (DPFT)				1.016	1.005	1.034	-	-	
			E_{10B}/E_{natB} (Eq.)				1.020	1.009	1.035	-	-	
3	-3	1	-0.25	0.25	0.25	43.9 ± 0.1	78.6 ± 0.2	125.6 ± 0.1	156.0 ± 0.3	-	c ^{nat} BN	
3	3	1	-0.25	-0.25	0.25	45.1 ± 0.1	80.5 ± 0.4	128.9 ± 0.2	158.1 ± 0.4	-	c ¹⁰ BN	
			E_{10B}/E_{natB} (experiment)				1.027(5)	1.024(7)	1.027(3)	1.014(4)	-	
			E_{10B}/E_{natB} (DPFT)				1.017	1.015	1.023	1.024	-	
			E_{10B}/E_{natB} (Eq.)				1.020	1.019	1.025	1.027	-	
3	-3	1	-0.1	0.1	-0.1	20.0 ± 0.1	33.8 ± 0.1	129.0 ± 0.5	160.2 ± 0.2	-	c ^{nat} BN	
3	1	1	-0.1	-0.1	-0.1	20.2 ± 0.1	34.2 ± 0.1	-	-	-	c ¹⁰ BN	
			E_{10B}/E_{natB} (experiment)				1.010(12)	1.012(8)	-	-	-	
			E_{10B}/E_{natB} (DPFT)				1.017	1.017	-	-	-	
			E_{10B}/E_{natB} (Eq.)				1.020	1.020	-	-	-	
3	-3	1	0	-0.5	-0.5	65.8 ± 1.1	85.6 ± 1.1	96.6 ± 1.1	126.7 ± 1.1	142.1 ± 1.4	c ^{nat} BN	
3	3	1	-0.5	0	0.5	66.8 ± 0.6	87.7 ± 0.3	99.0 ± 0.3	129.8 ± 0.2	144.7 ± 0.3	c ¹⁰ BN	
			E_{10B}/E_{natB} (experiment)				1.014(26)	1.025(17)	1.024(15)	1.025(11)	1.018(12)	
			E_{10B}/E_{natB} (DPFT)				1.016	1.017	1.015	1.024	1.023	
			E_{10B}/E_{natB} (Eq.)				1.020	1.021	1.019	1.026	1.025	
4	0	0	0	0.75	0.75	109.1 ± 0.3	-	-	121.1 ± 0.2	135.0 ± 0.8	c ^{nat} BN	
2	2	-2	0	0.75	-0.75	108.7 ± 0.4	-	113.8 ± 0.1	-	133.7 ± 0.2	c ^{nat} BN	
3	-3	1	-0.75	0.75	0	108.0 ± 0.4	109.6 ± 0.3	-	121.4 ± 0.1	134.5 ± 0.2	c ^{nat} BN	
4	0	0	0	0.75	0.75	111.2 ± 0.3	-	-	122.3 ± 0.2	138.1 ± 0.5	c ¹⁰ BN	
			E_{10B}/E_{natB} (experiment)				1.024(6)	-	-	1.008(3)	1.028(6)	
			E_{10B}/E_{natB} (DPFT)				1.018	-	-	1.017	1.031	
			E_{10B}/E_{natB} (Eq.)				1.026	-	-	1.020	1.032	
3	-3	1	0	0.25	-0.25	36.9 ± 0.2	45.7 ± 0.1	60.8 ± 0.2	127.8 ± 0.2	156.9 ± 0.2	c ^{nat} BN	
3	3	1	0	-0.25	-0.25	39.3 ± 1.4	46.7 ± 0.3	61.6 ± 0.4	130.6 ± 0.3	161.3 ± 0.3	c ¹⁰ BN	
			E_{10B}/E_{natB} (experiment)				1.065(42)	1.023(9)	1.013(9)	1.022(3)	1.028(4)	
			E_{10B}/E_{natB} (DPFT)				1.017	1.017	1.017	1.022	1.023	
			E_{10B}/E_{natB} (Eq.)				1.020	1.021	1.020	1.025	1.026	
4	0	0	-0.5	0	0	81.1 ± 0.3	-	-	-	-	c ^{nat} BN	
2	2	-2	0	0.65	0	71.1 ± 1.6	98.0 ± 1.7	119.5 ± 1.3	153.7 ± 1.3	-	c ^{nat} BN	
3	1	1	0.1	0	0	14.0 ± 1.0	18.3 ± 0.8	-	-	-	c ¹⁰ BN	
3	1	1	-0.17	-0.17	-0.17	34.1 ± 0.2	58.3 ± 0.3	-	-	-	c ¹⁰ BN	

phonons in cBN is 10 ~ 100 GHz, which seems almost independent of the phonon energy. From these values, the intrinsic linewidth of acoustic phonons can be estimated as 0.04 ~ 0.4 meV depending on the phonon propagation direction. In addition, isotope disorder reduces the lifetime further in c^{nat}BN. According to the calculations by Chen *et al.* [1], the isotope-phonon scattering rate is 0.2 GHz (for low-energy phonons) and ~300 GHz (for high-energy phonons). From the simple summation, the linewidth of high-energy phonons

in c^{nat}BN could be 1.7 meV (400 GHz). If taking the ratio of 1.85 given in the previous paragraph, the linewidth in c^{nat}BN would be 0.7 meV. In either case, the difference in the phonon linewidths between c¹⁰BN (0.4 meV) and c^{nat}BN (1.7 or 0.7 meV) could be observed in IXS spectra if the statistics of the spectra were high enough. However, we could not do that based on the present experimental results because of the large fitting uncertainties (see Table II). Higher-statistics IXS spectra near the zone boundary might elucidate the isotope

TABLE II. Experimentally determined phonon linewidth along high-symmetry lines. The values in bold are of acoustic modes.

H	K	L	h	k	l	ΔE (width) [meV]				sample		
2	2	-2	1	0	0	0.12 ± 0.11	0.19 ± 0.19	0.00 ± 0.08	0.65 ± 0.27	–	c ^{nat} BN	
3	1	1	1	0	0	0.07 ± 0.83	0.60 ± 0.61	0.51 ± 0.33	0.51 ± 0.30	–	c ¹⁰ BN	
			$\Delta E_{\text{natB}}/\Delta E_{10\text{B}}$				2 ± 25	0.3 ± 0.6	0.0 ± 0.2	1.3 ± 1.3	–	
3	1	-1	0	0	-0.3	1.03 ± 0.07	0.98 ± 0.49	0.54 ± 0.14	–	–	c ^{nat} BN	
1	3	1	0	0	0.3	0.87 ± 0.12	2.21 ± 0.89	0.32 ± 0.27	0.17 ± 2.04	–	c ¹⁰ BN	
			$\Delta E_{\text{natB}}/\Delta E_{10\text{B}}$				1.2 ± 0.2	0.4 ± 0.4	1.7 ± 1.8	–	–	
3	1	-1	-0.5	0.5	0.5	0.09 ± 0.20	0.43 ± 0.10	–	–	–	c ^{nat} BN	
4	0	0	-0.5	0.5	0.5	0.04 ± 0.05	0.09 ± 0.27	0.87 ± 2.07	–	–	c ^{nat} BN	
3	1	1	0.5	0.5	0.5	0.38 ± 0.24	0.46 ± 0.16	0.04 ± 0.34	–	–	c ¹⁰ BN	
			$\Delta E_{\text{natB}}/\Delta E_{10\text{B}}$				0.2 ± 0.4	0.6 ± 0.6	20 ± 208	–	–	
3	-3	1	-0.25	0.25	0.25	0.02 ± 0.40	1.13 ± 0.15	0.11 ± 0.14	1.28 ± 0.27	–	c ^{nat} BN	
3	3	1	-0.25	-0.25	0.25	1.03 ± 0.16	1.62 ± 4.00	0.00 ± 0.06	0.56 ± 0.87	–	c ¹⁰ BN	
			$\Delta E_{\text{natB}}/\Delta E_{10\text{B}}$				0.0 ± 0.4	0.7 ± 1.8	*	2.3 ± 4.0	–	
3	-3	1	-0.1	0.1	-0.1	0.76 ± 0.10	2.35 ± 0.11	1.22 ± 0.54	0.40 ± 0.15	–	c ^{nat} BN	
3	1	1	-0.1	-0.1	-0.1	1.31 ± 0.10	2.28 ± 0.12	–	–	–	c ¹⁰ BN	
			$\Delta E_{\text{natB}}/\Delta E_{10\text{B}}$				0.6 ± 0.1	1.0 ± 0.1	–	–	–	
3	-3	1	0	-0.5	-0.5	0.81 ± 0.34	0.46 ± 0.12	0.00 ± 0.16	0.81 ± 0.18	0.03 ± 0.09	c ^{nat} BN	
3	3	1	-0.5	0	0.5	1.22 ± 1.03	0.60 ± 0.40	0.08 ± 1.21	0.47 ± 0.34	0.00 ± 0.11	c ¹⁰ BN	
			$\Delta E_{\text{natB}}/\Delta E_{10\text{B}}$				0.7 ± 0.8	0.8 ± 0.7	0.0 ± 2.5	1.7 ± 1.6	*	
4	0	0	0	0.75	0.75	0.99 ± 0.29	–	–	0.44 ± 0.15	1.15 ± 0.95	c ^{nat} BN	
2	2	-2	0	0.75	-0.75	0.40 ± 0.39	–	0.02 ± 0.43	–	0.15 ± 0.20	c ^{nat} BN	
3	-3	1	-0.75	0.75	0	1.28 ± 0.15	0.06 ± 0.11	–	0.06 ± 0.77	0.41 ± 0.18	c ^{nat} BN	
4	0	0	0	0.75	0.75	0.95 ± 0.31	–	–	0.39 ± 0.24	0.73 ± 0.69	c ¹⁰ BN	
			$\Delta E_{\text{natB}}/\Delta E_{10\text{B}}$				0.9 ± 0.6	–	–	0.7 ± 1.6	0.8 ± 1.3	
3	-3	1	0	0.25	-0.25	0.87 ± 0.27	1.03 ± 0.18	1.26 ± 0.21	0.47 ± 0.16	0.48 ± 0.24	c ^{nat} BN	
3	3	1	0	-0.25	-0.25	3.51 ± 1.53	0.83 ± 0.45	0.81 ± 0.41	0.47 ± 0.31	0.06 ± 0.36	c ¹⁰ BN	
			$\Delta E_{\text{natB}}/\Delta E_{10\text{B}}$				0.2 ± 0.2	1.2 ± 0.9	1.6 ± 1.0	1 ± 1	8 ± 50	
4	0	0	-0.5	0	0	1.71 ± 0.17	–	–	–	–	c ^{nat} BN	
2	2	-2	0	0.65	0	0.21 ± 0.30	0.68 ± 3.42	0.10 ± 0.73	0.58 ± 0.17	–	c ^{nat} BN	
3	1	1	0.1	0	0	1.53 ± 0.41	1.58 ± 0.43	–	–	–	c ¹⁰ BN	
3	1	1	-0.17	-0.17	-0.17	2.56 ± 0.39	1.17 ± 0.21	–	–	–	c ¹⁰ BN	

*divided by zero.

effect on phonon lifetimes. It is also possible to consider using better (1.3 or even 0.8 meV) resolution but those setups have lower intensity, and would require rather long counting times

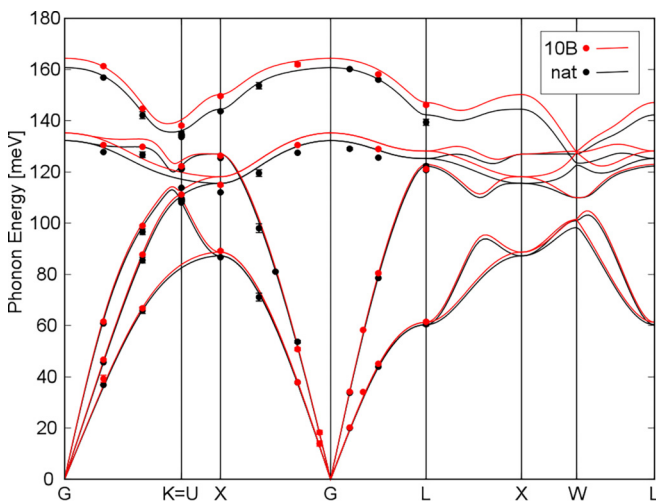


FIG. 3. Measured phonon dispersions for c¹⁰BN (red) and c^{nat}BN (black) given by spheres with error bars along some high-symmetric lines in Brillouin zone. Lines are calculated dispersion curves for c¹⁰BN (red) and c^{10.81}BN (black).

with these small samples. As for low-energy phonons, the isotope effect on the acoustic phonon linewidth (0.04 meV) would be difficult to observe because the contribution of the isotope disorder is small compared to the energy resolution of IXS (2.8 meV for the present setup or 1.4 meV in another typical setup).

IV. SUMMARY

We have investigated isotope effects on cBN. There was no significant difference in the XRS signals, but it did successfully detect an impurity phase of hBN in single-crystal-like grains. The effect of the mass difference well explains changes in phonon energies, and also phonon velocities. We also give an analytic expression for the isotope effect on the frequencies of phonons with any polarization in a multiatom primitive cell. While we did not see any significant phonon lifetime changes, the effect of isotope enrichment on the phonon lifetime may be observable with high-statistics spectra and/or better resolution.

ACKNOWLEDGMENT

We thank Dr. Wenyang Zhao for help during the meV-IXS data collection.

- [1] K. Chen, B. Song, N. K. Ravichandran, Q. Zheng, X. Chen, H. Lee, H. Sun, S. Li, G. A. Gamage, U. Gamage, F. Tian, Z. Ding, Q. Song, A. Rai, H. Wu, P. Koirala, A. J. Schmidt, K. Watanabe, B. Lv, Z. Ren, L. Shi, D. G. Cahill, T. Taniguchi, D. Broido, and G. Chen, Ultrahigh thermal conductivity in isotope-enriched cubic boron nitride, *Science* **367**, 555 (2020).
- [2] T. Taniguchi and S. Yamaoka, Spontaneous nucleation of cubic boron nitride single crystal by temperature gradient method under high pressure, *J. Cryst. Growth* **222**, 549 (2001).
- [3] T. Taniguchi and K. Watanabe, Synthesis of high-purity boron nitride single crystals under high pressure by using Ba–BN solvent, *J. Cryst. Growth* **303**, 525 (2007).
- [4] N. Hiraoka and Y. Q. Cai, High-pressure studies by x-ray raman scattering, *Synchrotron Radiat. News* **23**, 26 (2010).
- [5] A. Q. R. Baron, *Introduction to High Resolution Inelastic X-Ray Scattering I and II Synchrotron Light Sources and Free-Electron Lasers: Accelerator Physics, Instrumentation and Science Applications*, edited by E. Jaeschke, S. Khan, J. R. Schneider, and J. B. Hastings (Cham, Springer International Publishing, 2006, 2008), pp. 1643–1757, see also [arXiv:1504.01098](https://arxiv.org/abs/1504.01098).
- [6] A. Q. R. Baron, Status of the riken quantum nanodynamics beamline (BL43LXU): The next generation for inelastic x-ray scattering, *SPring-8 Inf.* **15**, 14 (2010), http://www.spring8.or.jp/pdf/ja/sp8-info/15-1-10/15-1-10-p14_press.pdf.
- [7] A. Q. R. Baron, D. Ishikawa, H. Fukui, and Y. Nakajima, Auxiliary optics for meV-resolved inelastic x-ray scattering at SPring-8: Microfocus, analyzer masks, Soller slit, Soller screen, and beam position monitor, *AIP Conf. Proc.* **2054**, 020002 (2019).
- [8] D. Ishikawa and A. Q. R. Baron, Practical measurement of the energy resolution for meV-resolved inelastic x-ray scattering, *J. Synchrotron Radiat.* **28**, 804 (2021).
- [9] P. Giannozzi, S. Baroni, N. Bonini, M. Calandra, R. Car, C. Cavazzoni, D. Ceresoli, G. L. Chiarotti, M. Cococcioni, I. Dabo, A. Dal Corso, S. de Gironcoli, S. Fabris, G. Fratesi, R. Gebauer, U. Gerstmann, C. Gougoussis, A. Kokalj, M. Lazzeri, L. Martin-Samos, N. Marzari, F. Mauri, R. Mazzarello, S. Paolini, A. Pasquarello, L. Paulatto, C. Sbraccia, S. Scandolo, G. Sclauzero, A. P. Seitsonen, A. Smogunov, P. Umari, and R. M. Wentzcovitch, QUANTUM ESPRESSO: A modular and open-source software project for quantum simulations of materials, *J. Phys.: Condens. Matter* **21**, 395502 (2009).
- [10] D. Vanderbilt, Soft self-consistent pseudopotentials in a generalized eigenvalue formalism, *Phys. Rev. B* **41**, 7892(R) (1990).
- [11] J. P. Perdew and A. Zunger, Self-interaction correction to density-functional approximations for many-electron systems, *Phys. Rev. B* **23**, 5048 (1981).
- [12] H. Fukui, A. Q. R. Baron, D. Ishikawa, H. Uchiyama, Y. Ohishi, T. Tsuchiya, H. Kobayashi, T. Matsuzaki, T. Yoshino, and T. Katsura, Pressure dependence of transverse acoustic phonon energy in ferropericlase across the spin transition, *J. Phys.: Condens. Matter* **29**, 245401 (2017).
- [13] M. Jaouen, G. Hug, V. Connet, G. Demazeau, and G. Tourillon, An EELS and XAS study of cubic boron nitride synthesized under high pressure–high temperature conditions, *Microsc. Microanal. Microstruct.* **6**, 127 (1995).
- [14] D. G. McCulloch, D. W. M. Lau, R. J. Nicholls, and J. M. Perkins, The near edge structure of cubic boron nitride, *Micron* **43**, 43 (2012).
- [15] A. Togo, L. Chaput, and I. Tanaka, Distributions of phonon lifetimes in Brillouin zones, *Phys. Rev. B* **91**, 094306 (2015).